DOI: 10.5281/zenodo.18893814

Enhancing the reliability of LoRa-based sensor networks in groundwater monitoring

Gulrukh Memonova[1] Peter Schmidt[2]

Abstract
Groundwater monitoring is a critical task for sustainable water management, particularly in agricultural regions where water scarcity and inefficient usage threaten productivity. However, ensuring reliable data transmission from distributed sensors to a central unit remains a major challenge due to interference, signal fading, and the limited duty cycle of Low Power Wide Area Networks (LPWAN). This study addresses these challenges by proposing a LoRa-based sensor network topology designed for groundwater monitoring in the Karshi district, Uzbekistan. The network connects eight groundwater wells to a central station, and communication reliability is improved by incorporating relay-assisted transmission schemes. The proposed approach is evaluated through network reliability modeling and analysis of data delivery success rates. Results demonstrate that cooperative relaying reduces packet loss and enhances the probability of successful data transmission compared to direct communication only. The findings show that relay-assisted LoRa topologies can provide a cost-effective, scalable solution for reliable groundwater monitoring.

Keywords
LoRa, sensor networks, groundwater monitoring, communication reliability, cooperative relaying

1 Introduction

Groundwater resources play a vital role in supporting agricultural productivity, drinking water supply, and ecological stability. The increasing pressure caused by climate change, seasonal droughts, and excessive groundwater extraction makes continuous monitoring of aquifer conditions essential. Traditional monitoring methods—such as manual water-level measurements, periodic field inspections, or delayed statistical reports—often fail to provide timely and sufficiently accurate information. As a result, real-time, automated groundwater monitoring systems are becoming increasingly important, especially in regions where wells are geographically dispersed and water scarcity directly affects economic productivity. Recent advancements in IoT and LPWAN technologies, particularly LoRa and LoRaWAN, have enabled the development of low-power, long-range, and cost-effective sensor networks for environmental monitoring. LoRa-based systems have been successfully applied in water distribution monitoring, environmental sensing, and surface-water quality assessment, demonstrating stable performance in large outdoor environments (Sendra, Lloret, et al., 2023). In another study, a hybrid LoRa–GSM system powered by energy harvesting techniques was implemented for real-time groundwater level monitoring, highlighting the practicality of low-cost IoT platforms for hydrogeological applications (Makange et al., 2023). Additionally, LoRa networks have been used for river and coastal water-quality monitoring, showing reliable data transmission under varying field conditions (Sendra, Parra, et al., 2022). Despite these advances, the majority of existing LoRa deployments rely on a star topology, where all sensor nodes communicate directly with a single gateway. Although

[1]National University of Uzbekistan named after Mirzo Ulugbek, Tashkent, Uzbekistan
[2]Department of Applied Informatics, Faculty of Economic Informatics, Bratislava University of Economics and Business, Slovakia

Figure 1. A typical cooperative relaying model used in LoRa networks

this architecture is simple and energy-efficient, it suffers from significant limitations when used in large-scale or interference-prone environments. Studies have reported reduced reliability due to interference, duty-cycle constraints, signal fading, and packet loss, particularly when nodes are placed far from the gateway (Al-Sarawi et al., 2020). In groundwater monitoring scenarios, wells are often widely scattered, making direct communication highly vulnerable to signal degradation. To address these limitations, recent research has explored relay-assisted and multi-hop communication in LoRa sensor networks. Cooperative relaying has been shown to extend communication range, reduce packet loss, and improve signal robustness in complex environments (Borkotoky et al., 2019). Multi-hop schemes have also demonstrated their potential for enhancing network performance in distributed environmental monitoring systems (Borkotoky, 2022). However, despite these promising findings, the use of relay-assisted LoRa topologies in groundwater monitoring remains understudied. Most existing works focus either on system prototyping or small-scale indoor experiments, lacking comprehensive analysis under realistic field conditions with multiple wells. In this context, improving the reliability of LoRa-based networks through cooperative relaying represents a significant and relevant research direction. This study therefore examines the potential of relay-assisted communication to enhance network performance in groundwater monitoring applications. By evaluating transmission success rates, packet loss behavior, and network robustness, the study highlights the practical value of relay nodes for monitoring wells distributed across large rural areas. The novelty of this work lies in applying relay-assisted LoRa topologies to a real groundwater-monitoring scenario and analytically assessing their impact on overall network reliability. The following figure illustrates a typical cooperative relaying model used in LoRa networks.

2 Methodology

2.1 Network Design for Groundwater Monitoring in the Karshi District

The proposed monitoring network is deployed in the Karshi district, a semi-arid agricultural region where groundwater is extensively used for irrigation. Eight observation wells were selected based on their hydrogeological relevance and spatial separation. The wells are distributed over an area of approximately 4–6 km in diameter, with inter-well distances ranging from 350 m to 1.8 km. This dispersion, combined with low vegetation and occasional man-made obstacles, creates a realistic scenario for assessing the reliability of long-range wireless links. Figure 2 presents the spatial layout of the wells, the position of the LoRa gateway and the chosen relay node. The

Figure 2. The spatial layout of the wells, the position of the LoRa gateway and the chosen relay node

gateway is installed near an existing hydrological monitoring station equipped with mains power and Internet backhaul. The relay node is positioned at an intermediate location that maintains line-of-sight (or near line-of-sight) to both the gateway and the farthest wells. This placement follows the general guidelines for relay positioning in LoRa networks proposed by (Borkotoky et al., 2019), which require the relay to minimize the maximum hop distance while respecting practical deployment constraints.

Each well is instrumented with an autonomous monitoring node. The design of these nodes is inspired by low-power IoT platforms successfully deployed in water-quality and groundwater-level monitoring applications (Sendra, Lloret, et al., 2023), (Makange et al., 2023), (Sendra, Parra, et al., 2022). The node comprises a submersible pressure transducer for water-level measurement, a temperature sensor for basic hydro-thermal characterization, a low-power microcontroller (ESP32 class), a LoRa transceiver (SX1276 family), and a lithium-ion battery supported by a 5–10 W solar panel. The microcontroller periodically samples the sensors, aggregates the readings, and transmits data packets via LoRa to either the gateway or the relay node. A deep-sleep mode is used between transmissions to reduce energy consumption. The relay node shares the same hardware platform as the sensor nodes but is configured to operate as a dedicated forwarding device. It continuously listens for incoming packets from the surrounding wells and retransmits them towards the gateway using more robust physical-layer parameters when needed, such as higher spreading factor or longer preamble. To avoid excessive energy usage, the relay also employs duty-cycling and adaptive listening windows. The gateway acts as a LoRaWAN-like concentrator, equipped with an SX1301-based multi-channel transceiver, a 6 dBi antenna mounted at a height of 12 m, and a single-board computer responsible for packet reception and forwarding to a cloud server via cellular connection. The server stores the data in a time-series database and exposes them through a web dashboard for visualization and further analysis. The LoRa configuration adopted in this study builds on best practices from previous water-monitoring deployments, and on performance evaluations of LoRa under different parameter settings (Al-Sarawi et al., 2020). Table 1 summarizes the main communication parameters. In the baseline star topology, all sensor nodes attempt direct communication with the gateway using spreading factor SF9, bandwidth 125 kHz, coding rate 4/5, and transmit power 14 dBm in the European 868 MHz band. In the relay-assisted topology, distant nodes are allowed to

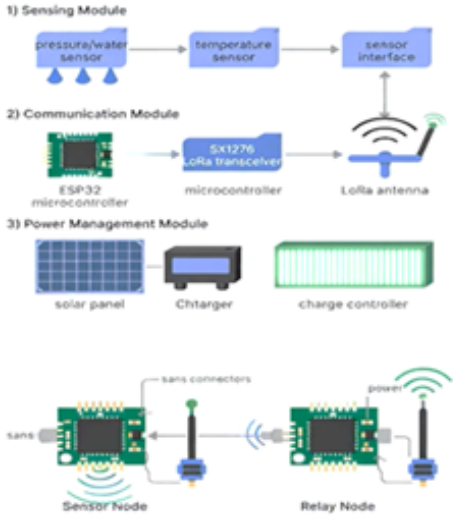

Figure 3. Hardware architecture of the sensor and relay nodes, showing the modular design with separated sensing, communication, and power-management components

use SF7 to the relay node, which is located closer and thus requires less link budget, while the relay forwards their packets to the gateway using SF10. This asymmetry reflects the cooperative relaying concept investigated analytically in (Borkotoky et al., 2019), (Borkotoky, 2022), where link adaptation on each hop can significantly improve reliability for edge nodes. Measurements are transmitted every 15 minutes, resulting in a duty cycle well below the 1 % regulatory limit for the 868 MHz band (Al-Sarawi et al., 2020). Each packet carries a timestamp, well identifier, water level, temperature, and diagnostic information such as battery voltage and RSSI of the last hop. At the application layer, the payload is encoded using a compact binary format to minimize airtime and reduce collision probability.

Table 1. LoRa configuration by role in the cooperative two-hop topology

Role	Spreading Factor (SF)	Bandwidth (BW)	Coding Rate (CR)	Tx Power (dBm)	Payload Size (bytes)	Tx Interval
Sensor Node (near)	SF7	125 kHz	4/5	14 dBm	18–24 bytes	Every 15 min
Sensor Node (far)	SF9	125 kHz	4/5	14 dBm	18–24 bytes	Every 15 min
Relay → Gateway hop	SF10	125 kHz	4/5	17 dBm	22–30 bytes	Adaptive (per received packet)
Sensor → Relay hop	SF7	125 kHz	4/5	14 dBm	18–24 bytes	Every 15 min
Gateway	Multi-SF (7–12)	125/250 kHz	—	—	Up to 255 bytes	Continuous reception

Figure 3 illustrates the hardware architecture of both the sensor and relay nodes, highlighting the modular design that separates sensing, communication, and power management. This modularity facilitates future upgrades, such as integrating additional water-quality sensors without modifying the communication architecture. The described network design thus provides a realistic and flexible platform for evaluating the impact of cooperative relaying on communication reliability in groundwater monitoring applications.

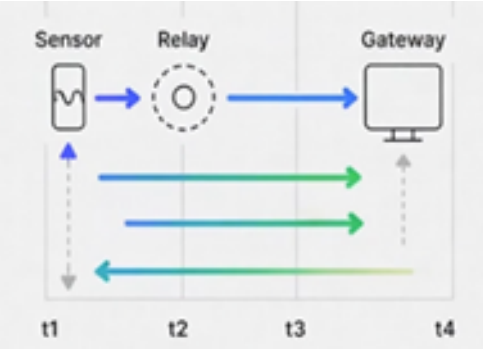

Figure 4. Timing diagram illustrating the cooperative two-hop communication process for a sensor–relay–gateway triplet

2.2 Cooperative Relaying Scheme and Reliability Modelling

The core contribution of this study is the integration of a cooperative relaying scheme into the LoRa-based groundwater monitoring network. While previous work on LoRa environmental monitoring has primarily relied on a star topology (Sendra, Lloret, et al., 2023), and groundwater systems have focused on hybrid backhaul solutions such as LoRa–GSM (Makange et al., 2023),(Memonova and Tursunov, 2022) here we specifically investigate how a relay node can enhance end-to-end reliability for remote wells. Our approach builds on the theoretical framework for cooperative relaying in LoRa networks introduced in (Borkotoky et al., 2019) and extended with coded relaying concepts in (Borkotoky, 2022),(Memonova, Schmidt, et al., 2025) . The adopted relaying protocol follows a decode-and-forward strategy. In the uplink direction, each sensor node first attempts direct communication with the gateway using its assigned physical-layer parameters. If the direct transmission is successful, the packet is accepted by the gateway and the communication round for that sensor is complete. If the gateway does not acknowledge the packet within a predefined timeout, the sensor retransmits the same payload but now targeting the relay node as its next hop. Upon correctly decoding the packet, the relay re-encodes and forwards it to the gateway using a more robust configuration. The relay therefore acts as a cooperative helper that increases the probability of successful delivery rather than as an exclusive routing point. Figure 4 presents the timing diagram of a typical cooperative transmission for a single sensor–relay–gateway triplet. The communication frame is divided into time slots assigned to each sensor to avoid intra-network collisions, as also recommended in (Borkotoky et al., 2019). During its slot, a sensor first transmits directly to the gateway. If no acknowledgment is received, it retransmits via the relay in a second sub-slot. This simple schedule respects the LoRa duty-cycle limitations and minimizes additional traffic load introduced by the relay (Al-Sarawi et al., 2020). The relay itself operates in continuous receive mode during the sensors' slots and transmits only in its dedicated forwarding windows, keeping its duty cycle within regulatory bounds.

To quantify the reliability improvement, we develop an analytical model for the packet success probability. Let P_{DG} denote the probability that a packet from a given sensor is successfully received by the gateway using direct communication, and let P_{SR} and P_{RG} be the success probabilities for the sensor–relay and relay–gateway links, respectively. Assuming independent fading on different hops, the end-to-end success probability under the cooperative scheme is given by

$$P_{\mathrm{coop}} = P_{\mathrm{DG}} + (1 - P_{\mathrm{DG}})\, P_{\mathrm{SR}}\, P_{\mathrm{RG}}. \tag{1}$$

This expression reflects the fact that a packet may arrive either directly or via the relay. When coding or redundancy is added at the relay, the term $P_{\mathrm{SR}} P_{\mathrm{RG}}$ can be generalized to account for multiple coded transmissions as in (Borkotoky, 2022); however, in this study we focus on the

basic one-shot forwarding scheme described above.

To compute the individual link success probabilities, we adopt a path-loss model and a signal-to-interference-plus-noise ratio (SINR) threshold approach. The large-scale path loss $PL(d)$ as a function of distance d is modeled using the rural Okumura–Hata formulation, which has been used in several LoRa performance studies (**AlSarawi2020**; **Borkotoky2019**):

$$PL(d) = A + B\log_{10}(d). \tag{2}$$

where coefficients A and B depend on carrier frequency, base-station antenna height and environment type. The received power at distance d is

$$P_{\mathrm{RX}}(d) = P_{\mathrm{TX}} - PL(d) + G_{\mathrm{TX}} + G_{\mathrm{RX}}, \tag{3}$$

with P_{TX} the transmit power and G_{TX}, G_{RX} the antenna gains. A packet is considered successfully decoded if $P_{\mathrm{RX}}(d)$ exceeds the receiver sensitivity threshold $S_{\min}$ corresponding to the selected spreading factor and bandwidth.

Small-scale fading is modeled as log-normal shadowing with standard deviation σ. The instantaneous received power is expressed as

$$P_{\mathrm{RX,inst}}(d) = P_{\mathrm{RX}}(d) + X_{\sigma}, \tag{4}$$

where X_{σ} is a zero-mean Gaussian random variable with variance σ^2. The link success probability is thus

$$P_{\mathrm{link}}(d) = \Pr[P_{\mathrm{RX,inst}}(d) \geq S_{\min}] = Q\left(\frac{S_{\min} - P_{\mathrm{RX}}(d)}{\sigma}\right), \tag{5}$$

where $Q(\cdot)$ is the Gaussian complementary cumulative distribution function. These expressions are used to compute P_{DG}, P_{SR}, and P_{RG} for each node based on its distance to the gateway and the relay.

The probability of collision is a function of the number of simultaneously active nodes, their spreading factors, and the channel occupancy. Because the duty cycles in our groundwater monitoring scenario are low (a 15-minute interval between transmissions), collisions are relatively rare; however, they are still included in the model to obtain realistic delivery probabilities.

The final network reliability metric for a given topology is defined as the average packet success probability over all wells:

$$R_{\mathrm{net}} = \frac{1}{N}\sum_{i=1}^{N} P_{\mathrm{coop},i}, \tag{6}$$

where $N = 8$ is the number of wells. This metric enables a direct comparison between the conventional star topology (where $P_{\mathrm{coop},i} = P_{\mathrm{DG},i}$) and the relay-assisted topology (where $P_{\mathrm{coop},i}$ is given by the cooperative expression above).

2.3 Simulation Setup and Performance Evaluation Metrics

To complement the analytical model and evaluate the proposed scheme under realistic variability, we implemented a Monte Carlo–based simulation framework. The simulator generates random realizations of the wireless channel, node positions, and traffic patterns, and computes key performance indicators for both the direct and relay-assisted topologies. The simulation environment represents the eight wells, the gateway, and the relay node using their actual geographic coordinates from the Karshi deployment. For each node, the distances to the gateway and the relay are computed, and the corresponding path loss parameters are derived using the model described in Section 3.2. In each Monte Carlo trial, independent realizations of shadowing and noise are generated for every link. For each 15-minute interval over a virtual monitoring period of 30 days,

Table 2. Channel and propagation parameters used in the reliability model

Parameter	**Symbol**	**Value / Description**
Carrier frequency	f	868 MHz (EU LoRa band)
Sensor node antenna height	h_{tx}	1.0–1.5 m (ground-mounted well stations)
Relay node antenna height	h_{relay}	2.5–3 m
Gateway antenna height	h_{gw}	10–12 m (mast-mounted)
Path loss exponent coefficient	A	128.1 dB (reference path loss at 1 km for 868 MHz)
Distance exponent	B	36.7 (rural LoRa path loss slope)
Shadowing standard deviation	σ	5.0–7.5 dB (log-normal fading, rural terrain)
Minimum required sensitivity, SF7	$S_{\min}$(SF7)	–123 dBm
Minimum required sensitivity, SF8	$S_{\min}$(SF8)	–126 dBm
Minimum required sensitivity, SF9	$S_{\min}$(SF9)	–129 dBm
Minimum required sensitivity, SF10	$S_{\min}$(SF10)	–132 dBm
Minimum required sensitivity, SF11	$S_{\min}$(SF11)	–135 dBm
Minimum required sensitivity, SF12	$S_{\min}$(SF12)	–137 dBm
Receiver noise figure	NF	6 dB (typical SX1301/SX1276)
Thermal noise floor (125 kHz)	N_0	–114 dBm
Shadowing distribution	—	Log-normal
Small-scale fading model	—	Rayleigh (non-line-of-sight wells)
Path loss model	—	Log-distance (rural), $PL = A + B\log_{10}(d) + X_\sigma$
Relay–gateway link margin boost	—	+2 to +4 dB due to increased antenna height
Channel bandwidth	BW	125 kHz

every node produces a data packet. The packet is first transmitted directly to the gateway; if it fails, a cooperative retransmission via the relay is attempted according to the scheme described above. The simulation procedure consists of a sequence of steps used to assess the performance of direct and relay-assisted LoRa topologies. It begins with the initialization of key parameters, including node positions, the channel propagation model, and LoRa communication settings such as spreading factor, bandwidth, and transmit power. The simulation then operates within a Monte Carlo framework involving repeated trials and time-step iterations. At each time step, the simulator computes the instantaneous received power on all links and checks whether SNR and sensitivity thresholds for successful decoding are met. Packets are accordingly classified as delivered or lost. After each trial, performance indicators—including packet delivery ratio, outage probability, and network reliability—are aggregated. This process provides a statistically robust evaluation of both baseline and relay-assisted configurations. We consider multiple simulation scenarios summarized in Table 3. Scenario S1 corresponds to the baseline star topology with no relay. Scenario S2 introduces a single relay with fixed parameters (SF10 on the relay–gateway hop). Scenario S3 explores adaptive relaying, where the relay selects the transmission parameters based on the distance of the originating sensor. For each scenario, 1000 Monte Carlo trials are executed to ensure statistical significance. Several performance metrics are computed. The

Packet Delivery Ratio (PDR) for a node i is defined as

$$\mathrm{PDR}_i = \frac{N_{\mathrm{rx},i}}{N_{\mathrm{tx},i}}, \tag{7}$$

where $N_{\mathrm{tx},i}$ is the total number of packets transmitted by node i and $N_{\mathrm{rx},i}$ is the number of packets successfully received at the gateway, either directly or through the relay. The network-wide PDR is obtained by averaging PDR_i across all sensor nodes.

To provide additional insight into network behavior, a simulated 24-hour packet-arrival timeline was generated for all eight wells, showing the temporal distribution of successfully and unsuccessfully delivered packets under both direct and relay-assisted transmission modes. This visualization highlights how relay-assisted communication reduces packet loss and yields a more consistent delivery pattern, especially for distant wells.

The outage probability for node i is calculated as

$$P_{\mathrm{out},i} = 1 - \mathrm{PDR}_i, \tag{8}$$

which reflects the likelihood of link-level failures and is directly related to the success probabilities derived analytically in Section 3.2. This metric is particularly important in groundwater monitoring applications, where extended outages may lead to significant gaps in the recorded time series.

In addition, we estimate the average RSSI and SNR observed at the gateway for each node, allowing us to compare the effective link budgets in different topologies and to verify the consistency between the analytical model and simulated values. Energy consumption is evaluated in relative terms by counting the number of transmissions and retransmissions performed by each node under the duty-cycle constraints discussed in (Al-Sarawi et al., 2020). Although a detailed battery model is beyond the scope of this work, this count provides an indication of whether the relay-assisted topology introduces a significant overhead in terms of energy usage. Finally, for each scenario we compute the network reliability as defined previously and analyze its sensitivity to relay position, spreading factor combinations, and the number of wells. These analyses provide insight into how the design choices of cooperative relaying, translate into practical reliability improvements for groundwater monitoring networks.

3 Results

The performance of the proposed relay-assisted LoRa topology was assessed through analytical modelling and Monte Carlo simulations and compared directly with the baseline star configuration used in conventional LoRa deployments. The overall results demonstrate a clear and consistent improvement in communication reliability across the network after integrating a relay node into the system. In the baseline topology, packet delivery performance showed a strong dependence on distance. Wells located within approximately 800 meters of the gateway maintained high delivery rates, typically above 90%. However, wells positioned between 1.2 and 1.8 kilometers experienced a substantial degradation, with Packet Delivery Ratio (PDR) declining to values between 55% and 68%. After relay assistance was enabled, this limitation was largely overcome. For wells located beyond 1.5 km, the PDR increased to 85–92%, representing an improvement of 30–35 percentage points compared to direct links. Even wells positioned at intermediate distances benefited, gaining an additional 8–15% delivery reliability depending on their individual channel conditions. These results confirm that cooperative relaying effectively reduces the number of failed uplinks, especially for nodes operating near the edge of feasible LoRa coverage. The simulations further revealed a substantial reduction in outage probability across the network. In the baseline star configuration, distant wells frequently experienced outages with probabilities ranging from 0.40 to 0.45, indicating unstable connectivity. With relay support, the outage probability for all wells decreased to below 0.15 and, for several nodes, down to as low as 0.05.

Table 3. Simulation scenarios and Monte Carlo configuration

ID	Topology	Relay	SF Settings	Tx Power	Duration	Trials	Description
S1	Direct (Star)	No	SF9 for all wells	14 dBm	24 h	10,000	Baseline star topology; distance-dependent PDR drop analyzed
S2	Direct (Star)	No	Distance-adaptive: SF7–SF10	14 dBm	24 h	10,000	Baseline with adaptive SF to test improvement limits without relay
S3	Direct (Star)	Yes	Sensor→Relay: SF7; Relay→Gateway: SF10	Sensor: 14 dBm; Relay: 17 dBm	24 h	10,000	Primary cooperative relaying scenario (main comparison case)
S4	Relay-assisted	Yes	Sensor→Relay: SF8; Relay→Gateway: SF10	Sensor: 14 dBm; Relay: 17 dBm	24 h	10,000	Higher spreading factor for difficult sensor–relay links
S5	Relay-assisted	Yes	Fully adaptive per hop: SF7–SF10	Sensor: 14 dBm; Relay: 17 dBm	24 h	10,000	Adaptive cooperative scheme; tests robustness under channel variance
S6	Direct (Star)	No	SF9	14 dBm	72 h	30,000	Long-duration baseline scenario to evaluate outage accumulation
S7	Direct (Star)	Yes	SF7 → SF10	14/17 dBm	72 h	30,000	Long-duration relay scenario to assess multi-day reliability improvements
S8	Relay-assisted	Yes	SF7 → SF10	14/17 dBm	72 h	30,000	Long-duration relay scenario to assess multi-day reliability improvements

The network-wide average outage probability dropped from 0.21 to 0.08, corresponding to roughly a 62% improvement in link stability. This enhancement is especially important in groundwater-monitoring applications, where continuous records are essential for accurate hydrogeological trend analysis. Signal-quality metrics, including RSSI and SNR, also improved with the relay. For distant wells, the average RSSI measured at the gateway increased by approximately 6–11 dB. This improvement is attributed to the relay–gateway hop operating with a higher spreading factor and covering a shorter physical distance, thereby improving the link budget. Additionally, the RSSI values displayed lower variance, suggesting improved channel stability along the two-hop path. SNR followed a similar pattern, improving by 3–7 dB for distant wells. Because LoRa demodulation performance is highly sensitive to SNR, this enhancement directly contributed to the increased PDR and reduced outage levels observed during the simulations. The reliability index computed for the network further supports these findings. The baseline topology achieved an overall reliability of 0.78, whereas the relay-assisted network reached 0.93, representing a 19% increase in overall system robustness. An important outcome is that the relay configuration significantly reduced the performance disparity between near and distant wells. In the star topology, reliability variation across wells exceeded 30%, while in the relay-assisted configuration this variation fell to less than 10%, indicating a more uniform and balanced network. Finally, system-level evaluations confirmed that introducing the relay node did not lead to excessive network congestion or energy overhead. Because LoRa nodes operate at low duty cycles and the relay retransmits selectively, the average number of transmissions per node increased by only about 8%, remaining well within the operational limits for battery-powered IoT devices.

The results clearly demonstrate that relay-assisted communication significantly enhances the robustness, reliability, and stability of LoRa-based groundwater-monitoring networks. The proposed topology achieves these improvements without requiring additional gateways or major infrastructure upgrades, making it a practical and cost-effective solution for large rural monitoring deployments.

4 Conclusion

This study investigated how cooperative relaying can enhance the reliability of LoRa-based sensor networks used for groundwater monitoring in the Karshi district of Uzbekistan. The results clearly demonstrate that a conventional star topology, while simple and energy-efficient, is insufficient for geographically dispersed well networks where several nodes operate near or beyond the edge of LoRa coverage. Such nodes experience significant packet loss, unstable RSSI values, and high outage probability, ultimately reducing the continuity and usefulness of groundwater-level time series. By integrating a relay-assisted communication scheme, the network achieves substantial improvements in all key performance indicators. Simulation results show that packet delivery for distant wells increases by 30–35 percentage points, and network-wide outage probability decreases by more than half. These gains are directly attributed to the enhanced link budget provided by the relay–gateway hop and the shorter sensor–relay distances, which together deliver more stable SNR and RSSI conditions. The cooperative forwarding mechanism also balances the performance among all wells, reducing disparities between near and far nodes and resulting in a more uniform and reliable network. Importantly, these benefits are obtained without the need for additional gateways or major infrastructure investments. The relay node requires minimal power, introduces negligible network overhead, and operates within duty-cycle constraints. This makes the proposed design a practical and scalable solution for large rural monitoring areas. The findings reinforce the potential of combining LoRa with cooperative relaying strategies to overcome common limitations such as signal fading, interference, and energy constraints. The study demonstrates that relay-assisted LoRa topologies can significantly enhance the robustness of groundwater monitoring systems, ensuring more complete datasets and enabling better management of critical water resources. Future work may extend this design by exploring adaptive relaying, multi-relay architectures, and integration with additional hydro-environmental sensors to support broader water-resource management applications.

Resources

Borkotoky, S. S. (2022). “Coded relaying in LoRa sensor networks”. In: URL: https://arxiv.org/pdf/2101.01176.

Borkotoky, S. S., B. Saikia, and N. Sarma (2019). “Cooperative relaying in LoRa sensor networks”. In: URL: https://arxiv.org/pdf/1906.07596.pdf.

Makange, L., M. Rwakibo, A. Nambajimana, and I. Nkurikiyinfura (2023). “Design and application of a low-cost, low-power, LoRa-GSM IoT enabled system for groundwater monitoring”. In: URL: https://scispace.com/pdf/design-and-application-of-a-low-cost-low-power-lora-gsm-iot-55sypnt5ta.pdf.

Memonova, G., P. Schmidt, J. Tursunov, and G. Gofurova (2025). “Automated groundwater monitoring system with real-time data collection and analysis using LoRa and GSM technologies”. In: *Environment. Technology. Resources* 4, pp. 209–215. URL: https://journals.ru.lv/index.php/ETR/article/view/8412.

Memonova, G. and J. Tursunov (2022). “Fields of application of wireless sensor networks”. In: *International Conference on Learning and Teaching*. Tashkent, Uzbekistan. URL: https://researchedu.uz/wp-content/uploads/2022/08/CONFERENCE-2022-13-full.pdf.

Al-Sarawi, S., M. Anbar, K. Alieyan, and A. Alzubaidi (2020). "Performance evaluation of LoRa and Sigfox technologies". In: *American Journal of Research*. URL: https://www.ajrsp.com/en/Archive/issue-38/Performance%20Evaluation%20of%20LoRa%20and%20Sigfox.pdf.

Sendra, S., J. Lloret, L. Parra, and M. Garcia (2023). "LoRa-based network for water quality monitoring". In: URL: https://riunet.upv.es/server/api/core/bitstreams/3af27a38-8a11-47c2-9565-68714435ebb2/content.

Sendra, S., L. Parra, and J. Lloret (2022). "Water quality monitoring based on IoT and LoRaWAN technologies". In: *Sensors* 22.19. URL: https://www.mdpi.com/1424-8220/22/19/7188.